Optics Communications 508 (2022) 127769

Contents lists available at ScienceDirect

Optics Communications

journal homepage: www.elsevier.com/locate/optcom

Simulation of highly sensitive temperature sensing based on a selectively ethanol-filled twin-core photonic crystal fiber

Xu Wang, Xiangying Hao, Shun Wu *

Hubei Key Laboratory of Optical information and Pattern Recognition, Wuhan Institute of Technology, Wuhan 430205, China

ARTICLE INFO

Keywords:
Photonic crystal fiber
Temperature sensing
Selectively ethanol-filled
Two-core fiber

ABSTRACT

A selectively ethanol-filled twin-core photonic crystal fiber (TC-PCF) sensing scheme is proposed and theoretically investigated for highly sensitive temperature sensing. Different filling cases and fiber structure were simulated to investigate the mode coupling of two solid fiber cores of the TC-PCF. Our calculation for the sensing performance shows that with properly designed fiber structure and filling configuration, a high temperature sensitivity of −16.7 nm/°C could be achieved in a range from 20 to 50 °C.

1. Introduction

Photonic crystal fiber (PCF) is a type of micro-structured optical fiber which has an array of air holes on the silica background [1]. PCF has many important applications in the fields of biology [2], medicine [3], and tele-communication [4] due to its designable structure and unique optical characteristics, such as engineered dispersion, large mode field area, high birefringence, and etc. Recent PCF-based sensors reported show promising results, which are highly sensitive to environmental changes including gas concentration [5], refractive index [6], curvature [7], gas pressure [8], as well as bending [9] and temperature sensing [10]. Among them, temperature sensing has been attracting great research interests.

Twin-core photonic crystal fiber (TC-PCF) is a special design of microstructure PCF and has two solid cores separated by the centered air-hole. By filling specified liquid into different air holes of fiber cladding, the coupling properties of the two cores can be changed to realize high sensitivity temperature sensing. As the PCF fabrication and multi-step infiltration technologies are developed, many temperature sensors based on the selectively-liquid-filled TC-PCF have been proposed. In 2016, Liu et al. demonstrated a fiber-optic dual parameter sensor based on a water-filled TC-PCF, where the average temperature sensitivity is 1.23 nm/°C [11]. In 2018, Xu et al. reported a temperature sensor based on the hybrid guiding mechanism, which is realized by selectively infiltrating liquid crystal 5CB into a TC-PCF. The average temperature sensitivity can achieve 4.75 nm/°C [12]. In 2015, Khurram et al. achieved a highly sensitive temperature sensor based on an all-fiber Mach–Zehnder interferometer using a selectively polymer-filled TC-PCF, where the average temperature sensitivity in the detection range of 25 to 100 °C is 1.595 nm/°C [13]. In 2020, Qiu et al. Proposed an all-solid cladding dual-core photonic crystal fiber (DC-PCF) filled with toluene and ethanol for temperature sensing. Light is confined in the two largest cores, so it can act as a TC-PCF. The average calculated sensitivity in the detection range of 0 to 70 °C is −11.64 nm/°C and −7.41 nm/°C from −80 to 0 °C [14]. However, in their simulation, they ignore the group effective index of refraction, which is an essential parameter when studying the transmission spectrum [13,15].

In this paper, we proposed a selectively ethanol-filled temperature sensor based on TC-PCF, in which the group effective index of refraction is considered in the simulation. With optimized hollow-core structural parameters, and ethanol filled into selected air holes, high sensitivity can be achieved for temperature sensing. Specifically, we investigated three tuning parameters for different filling cases: (1) the size of the solid twin cores, (2) the number of the filling layers around the core, and (3) the ratio between the radius of the air hole and the distance between two adjacent air holes, denoted as d and Λ, respectively. The temperature performances for different filling configurations are numerically studied by the finite element method (FEM). Our results show that the maximum temperature sensitivity can achieve −16.7 and −14.18 nm/°C in the temperature range of 20 to 50 °C.

2. Theory

The cross-sectional structure of the proposed unfilled TC-PCF is displayed as Fig. 1. It is formed by a triangular lattice of circular air holes with two solid fiber cores (A and B). The structure is not circular symmetric, a row of air holes near the two cores on the x-axis are deviated few μm from their original position. Diameter of the two cores in the transverse direction is 5.47 μm. The radius of the air holes d is 1.78 μm. The distance between the two adjacent air holes Λ is 4.9 μm. We found the temperature sensing performance can be greatly

* Corresponding author.
E-mail address: wushun@wit.edu.cn (S. Wu).

https://doi.org/10.1016/j.optcom.2021.127769
Received 9 August 2021; Received in revised form 3 December 2021; Accepted 5 December 2021
Available online 13 December 2021

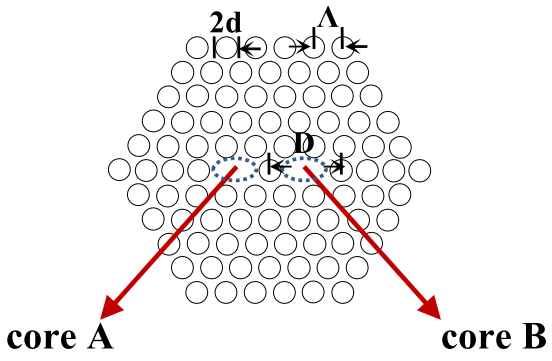

Fig. 1. The simulated cross-section of the proposed TC-PCF.

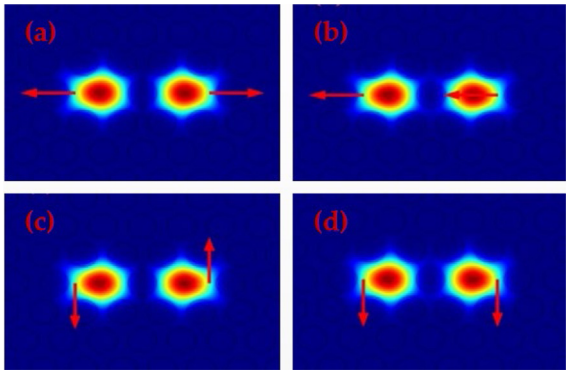

Fig. 2. Distribution of the four supermodes in the proposed dual core PCF. Arrows represent the polarization direction: **(a)** the x-polarized odd mode **(b)** the x-polarized even mode **(c)** the y-polarized odd mode **(d)** the y-polarized even mode.

enhanced by selective filling ethanol to the air holes near the fiber cores. This is because the temperature sensitivity of the TC-PCF are fundamentally determined by the thermo-optic (TO) mismatch between the interfering modes. Selectively filling the air holes surrounding the fiber cores can induce a large mismatch in the TO property between the cores, which thus improve the temperature sensitivity.

We use COMSOL to investigate the guide modes and temperature sensing characteristics of the TC-PCF. The refractive index of silica is governed by the Sellmeier equation [16]:

$$n_{silica} = \sqrt{1 + \frac{0.6961663\lambda^2}{\lambda^2 - 0.068043^2} + \frac{0.4079426\lambda^2}{\lambda^2 - 0.1162414^2} + \frac{0.8974794\lambda^2}{\lambda^2 - 9.896161^2}} \quad (1)$$

The refractive index of ethanol $n_{ethanol}$ is calculated through the following equation [17]:

$$n_{ethanol} = \sqrt{1 + \frac{0.0165\lambda^2}{\lambda^2 - 9.08} - \frac{0.8268\lambda^2}{\lambda^2 - 0.01039}} - \alpha(T - 20) \quad (2)$$

where λ is wavelength in μm, T is temperature in °C, and α is the thermo-optic of ethanol. $\alpha = 3.98 \times 10^{-4}/°C$.

Two fiber cores can be regarded as two independent waveguides. There also exist two supermodes (odd and even mode), which are formed by coupling the individual core mode in the corresponding polarization direction. Fig. 2(a–b) show the electric field amplitude and electric field vector of the odd and even mode in x-polarization at 1550 nm, respectively, while Fig. 2(c–d) show that in y-polarization.

Based on the mode coupling theory [15], the interference between two supermodes in the same polarization state causes periodic optical power coupling from one core to the other along the fiber. The physical quantity that characterizes the periodic coupling is called the coupling length L_c. Only when the polarization state of the two supermodes are orthogonal to each other, there is no power coupling between them.

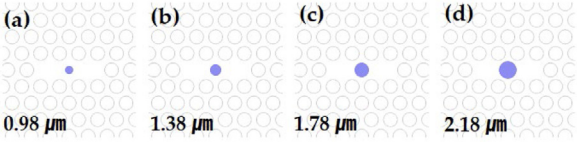

Fig. 3. The cross-sectional image of the TC-PCF when only the central air hole is filled with ethanol. The diameter of the central holes are set as **(a)** 0.98 μm, **(b)** 1.38 μm, **(c)** 1.78 μm, **(d)** 2.18 μm, respectively.

The coupling length L_c^i in x-polarization or y-polarization is given by [18,19]:

$$L_c^i = \frac{\lambda}{2\left|\left(n_o^i - n_e^i\right)\right|} = \frac{\lambda}{2\Delta n} \quad i = x, y \quad (3)$$

Here, n_o^i and n_e^i are the effective refractive indices of the odd modes and even modes in i-polarization, respectively. Δn represents the difference between n_o^i and n_e^i. Consider practical applications, Δn should be replaced by ΔN, which is the difference between the group effective index of refraction of the odd and even modes. Simulations using ΔN are reported to agree better with the experimental results [13,15]. ΔN can be described as follows [20]:

$$\Delta N = \Delta n - \lambda \frac{\partial \Delta n}{\partial \lambda} \quad (4)$$

If the input light is launched into the fiber core A, the optical power which is transferred into core B can be given by [21]:

$$I(\lambda) = \sin^2\left(\frac{\pi}{2L_C}L\right) = \sin^2\left(\frac{\pi \Delta N}{\lambda}L\right) \quad (5)$$

ΔN varies along with the temperature, resulting in the wavelength shift for the interference dips in the transmission spectrum. The wavelength shift for interference peaks due to the variation of temperature reflects the sensitivity of temperature sensing, which can be defined as [22]:

$$S\,(\mathrm{nm}/°\mathrm{C}) = \frac{\partial \lambda_{peak}}{\partial T} \quad (6)$$

3. Simulation results and discussion

We investigated the temperature sensing performances for three different ethanol-filling cases: (1) only the central hole is filled, (2) one, two or three layers of the central ring is filled, and (3) a single layer of the central ring is filled, however, with different spacing between microstructure holes. These filling configurations are represented by Figs. 3, 5 and 6. We will discuss these results in the following paragraphs.

Fig. 3(a–d) shows the cross-section of the first filling case. Only the central air core is filled with ethanol, while the radius of the core is 0.98 μm, 1.38 μm, 1.78 μm, 2.18 μm, respectively. In the simulation, we optimized the length of TC-PCF to make the spectrum peak appear near 1550 nm when the parameters are changed.

Fig. 4(a) shows the transmission spectra of the y-polarized light in the temperature range of 20 to 50 °C when the core radius is 0.98 μm. The refractive index of the ethanol decreases with the increase of temperature. When temperature increases, the refractive index of silica does not vary much. On the contrary, the refractive index of ethanol decreases substantially, which results in the increasing of coupling length in y-polarized direction. According to Eq. (5), this leads to blue-shift for the interference dip [23].

Fig. 4(b–c) shows the wavelength shift of interference dips for cases with different core diameters, in temperature range of 20 to 50 °C. The peak wavelength is found to be decreasing linearly with temperature. Four different core sizes are studied, with the corresponding sensitivities and fiber length shown in the Figure. From Fig. 4(c), as the radius increases from 0.98 to 2.18 μm, the blue-shift becomes larger and the sensitivity increases from −6.25 nm/°C to −16.7 nm/°C. Our

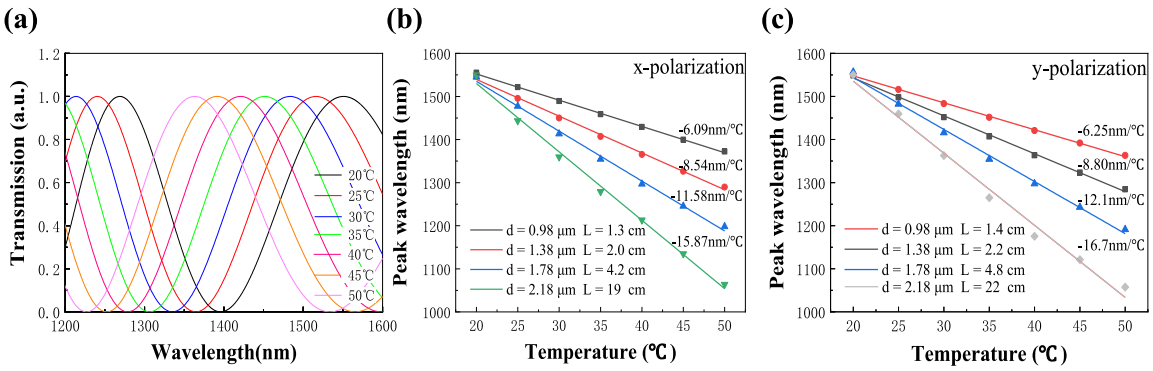

Fig. 4. **(a)** The transmission spectra of the y-polarized light in the temperature range of 20 to 50 °C when the diameter is 0.98 μm; The peak wavelength of different diameters in the temperature range of 20 to 50 °C for **(b)** x-polarization, and **(c)** y-polarization.

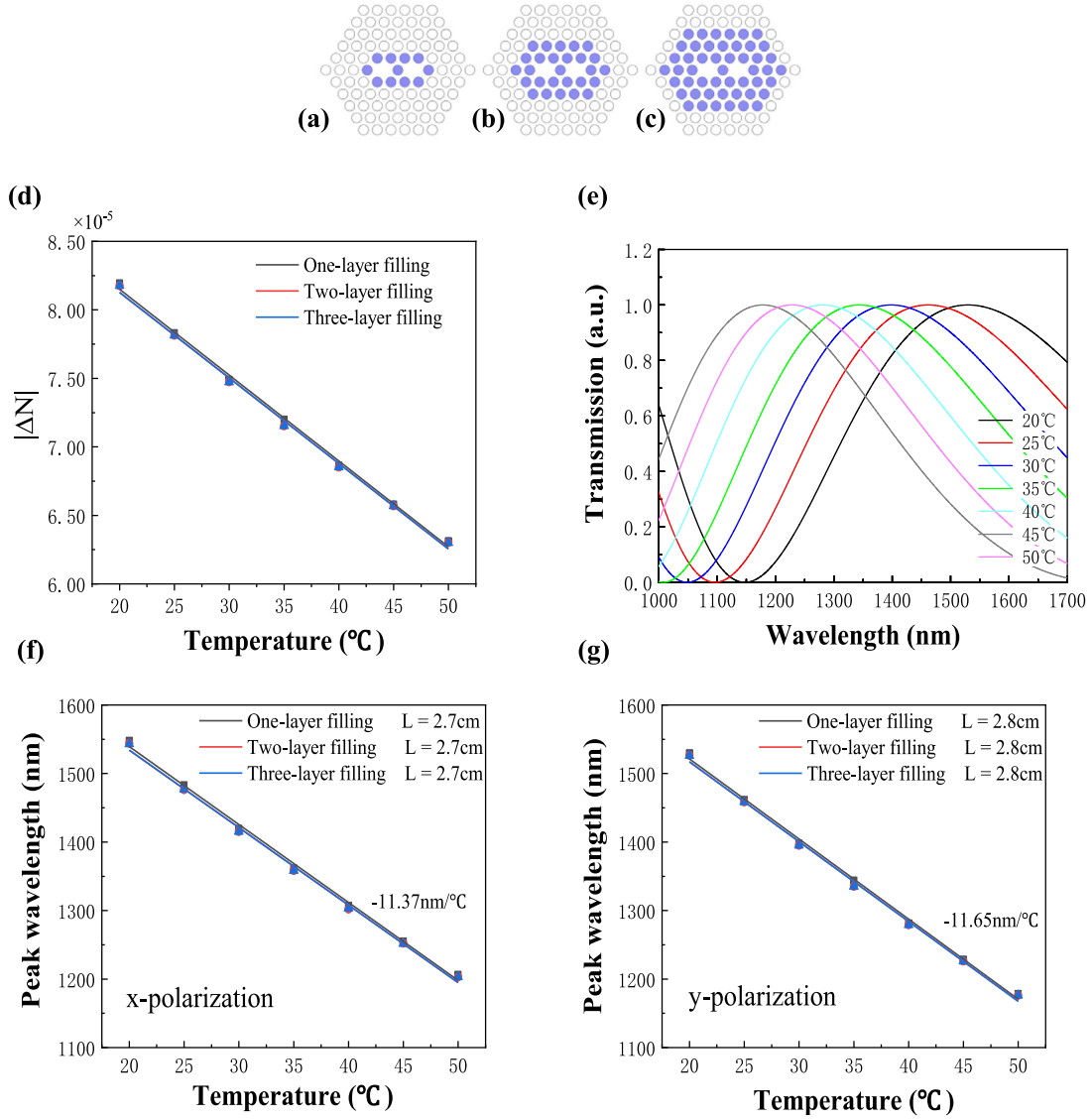

Fig. 5. Cross-sectional of the TC-PCF. **(a)** one, **(b)** two, and **(c)** three layers of air hole filled with ethanol. **(d)** Difference between the group effective index of refraction of the odd and even modes in y-polarization; **(e)** The transmission spectra of the y-polarized light in the temperature range of 20 to 50 °C with one layer of filling; The peak wavelength for different layers of filling in the temperature range of 20 to 50 °C for **(f)** x-polarization; **(g)** y-polarization.

result shows that it is feasible to improve the temperature sensitivity by increasing the diameter of the central air hole for the first filling case.

Fig. 5(a–c) shows the cross-section of the second filling case. Selective filling can be accomplished by blocking the holes which do not require to be filled by UV glue, and followed by the liquid-filling to the open holes. Detailed description can be found in Ref. [24]. In the simulation, we filled the first one, two, or three layers of air holes around the core with ethanol. Our result shows that the wavelength of

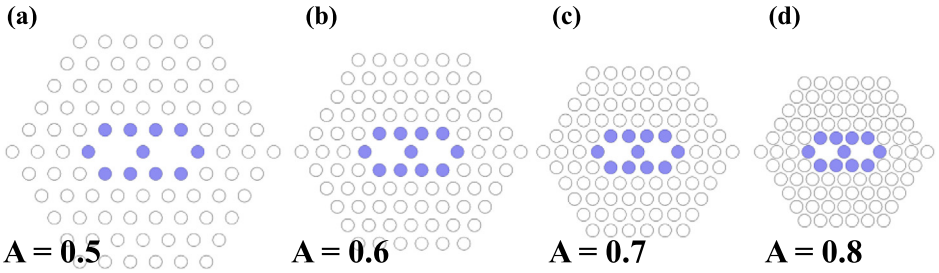

Fig. 6. Cross-sectional of the TC-PCF. **(a)** A is 0.5; **(b)** A is 0.6; **(c)** A is 0.7; **(d)** A is 0.8.

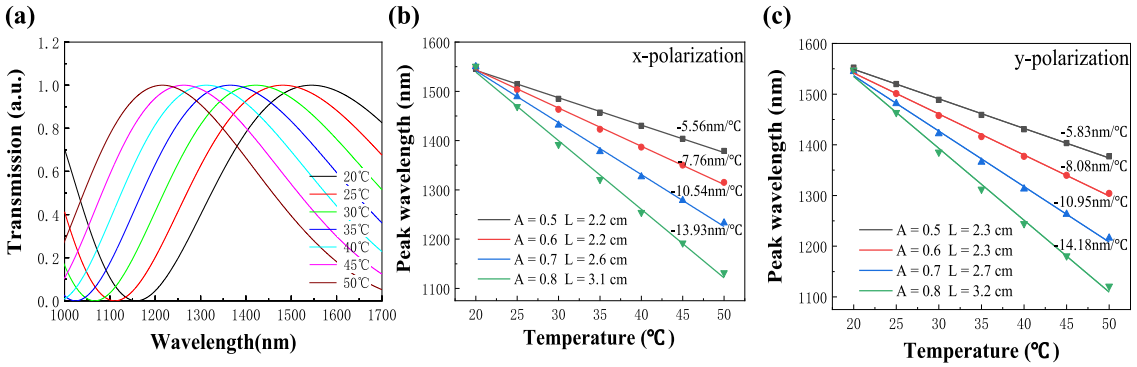

Fig. 7. **(a)** The transmission spectra of the y-polarized light in the temperature range of 20 to 50 °C when the A is 0.7; The peak wavelength of different A in the temperature range of 20 to 50 °C for **(b)** x-polarization, and **(c)** y-polarization.

the interference peaks decreases linearly with temperature for all cases. The rate of change is almost identical. Fig. 5(e) shows the transmission spectra of the y-polarized light in the temperature with one layer of filling. Similar to the result shown in Fig. 4(a), the peak wavelength at the same temperature also experiences blue-shift. Fig. 5(f–g) indicates the peak wavelength decreases linearly with a similar sensitivity of −11.65 nm/°C for all three filling cases. The length of the fiber is optimized to be 2.8 cm. Our result shows that the sensing behavior is similar for filling single or multiple layers. It indicates that ethanol in the first layer has a strong effect of alter altering the coupling characteristics, while the ethanol in the outer layers have minor effect.

Fig. 6(a–d) shows the third filling configuration. We define A as the ratio of $2d/\Lambda$. As we change the value of A, we always fill the first layer of air holes with ethanol.

Fig. 7(a) illustrates the transmission spectra of the y-polarized light in the temperature range of 20 to 50 °C when A is 0.7. From Fig. 7(a), as the temperature increases, the interference peaks exhibit blue shift. Fig. 7(c) shows the peak wavelength for different values of A. As shown in the figure, the wavelength decreases linearly with temperature. When A is 0.5, 0.6, 0.7, 0.8, the temperature sensitivity is −5.83 nm/°C, −8.08 nm/°C, −10.95 nm/°C, −14.18 nm/°C, respectively. In the calculation, the length of the TC-PCF is set as 2.3 cm, 2.3 cm, 2.7 cm, 3.2 cm, respectively. It is found that the temperature performance can be improved by increasing the ratio of $2d/\Lambda$.

The temperature sensing performances for three different ethanol-filling cases in the x-polarization were also calculated. Compared with the sensitivity in y-polarization, the sensitivity in x-polarization for all cases are slightly smaller, within 5 percent. It indicates that y-polarized modes should be considered for better temperature sensing performances.

We compare our results to other reported work with selectively filled PCF configurations in Table 1. It can be seen that our proposed sensor has a high temperature sensitivity.

In practical applications, confinement loss [25] can be a limiting factor to achieve interference fringes with high contrast ratio. Therefore, we investigated how confinement loss increases with temperature. Since the refractive index of ethanol is lower than that of silica, large-area filling of ethanol may increase the loss of the fiber.

Table 1
Comparison between the proposed PCF temperature sensing with other reports.

Ref.	Sensing principle	Temperature detection range (°C)	Sensitivity (nm/°C)
[11]	Water-filled TC-PCF	20–50	1.23
[12]	Liquid crystal-filled TC-PCF	27–31	4.75
[13]	Polymer-filled TC-PCF	25–100	1.595
[14]	Dual-core toluene and ethanol filled PCF	0–70 −80–0	11.64 7.41
[24]	Toluene-filled PCF	−80–90	6.02
[26]	Oil-filled PCF	30–150	0.61
This work	Ethanol-filled TC-PCF	20–50	16.7 11.65 14.18

In the first and second filling case, the confinement in the wavelength range of 1.1 μm to 1.6 μm were calculated to be on the order of 10^{-14} and 10^{-13} dB/cm, respectively. Light is tightly confined to the fiber core by the first layer of air hole, while the radius of the central core or number of filling layers have minor effect on the confinement loss. In the third filling case, the value of A has strong effect on confinement loss. When A is 0.5, 0.6, 0.7 0.8, the loss is found to be on the order of 10^{-9}, 10^{-12}, 10^{-13}, and10^{-14}dB/cm, respectively. Fig. 8 shows the confinement loss when A is 0.5 and 0.6. We can see that the confinement loss increases with wavelength and decrease with A. The above discussion indicates the confinement loss in all cases are quite low. Thus, the proposed TC-PCF filling scheme is practical.

4. Conclusions

In summary, we proposed a selectively ethanol-filled TC-PCF for highly sensitive temperature sensing. Three different filling cases were simulated to investigate the temperature sensing performance. When only the central air core is filled with ethanol, the temperature sensitivity increases with the diameter of the core and the maximum sensitivity obtained in our simulation is −16.7 nm/°C when the core diameter is 2.18 μm. Our result also indicates that the sensing behavior is almost identical for filling single or multiple surrounding layers, which is

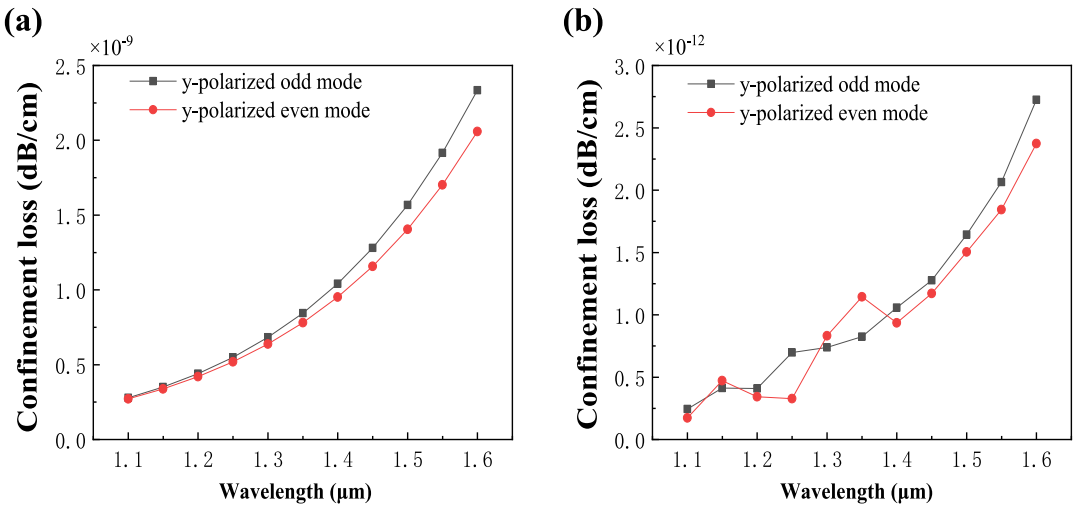

Fig. 8. The confinement loss of the y-polarized modes in the wavelength rang of 1.1 μm to 1.6 μm when A is **(a)** 0.5; **(b)** 0.6.

−11.65 nm/°C. In addition, the temperature sensitivity increase with the ratio of d/Λ while the first layer of air holes are filled with ethanol. When the ratio is 0.8, the temperature sensitivity can achieve −14.18 nm/°C. The temperature ranges is from 20 to 50 °C for all the above calculations.

Compared to other reported simulation work regarding temperature sensing performance of selectively filled PCF configurations [14], we consider the group effective index of refraction in our simulation. Our scheme has combined advantages of high sensitivity and simple structure, which made the proposed TC-PCF sensor a strong candidate in optical fiber temperature sensing applications.

Declaration of competing interest

The authors declare that they have no known competing financial interests or personal relationships that could have appeared to influence the work reported in this paper.

Acknowledgments

This research was funded by National Natural Science Foundation of China (NSFC) [grant number 61805182], and Campus Science Foundation of Wuhan Institute of Technology, China [grant number 18QD19].

References

[1] P.S.J. Russell, Photonic-crystal fibers, J. Lightwave Technol. 24 (2006) 4729–4749.
[2] P. Marc, N. Przybysz, A. Molska, L.R. Jaroszewicz, Photonic crystal fiber transducers for an optical fiber multilevel temperature threshold sensor, J. Lightwave Technol. 36 (2018) 898–903.
[3] M.M.A. Eid, M.A. Habib, M.S. Anower, A.N.Z. Rashed, Hollow core photonic crystal fiber (PCF)–based optical sensor for blood component detection in Terahertz spectrum, Braz. J. Phys. (2021).
[4] Y. Gao, C. Sima, J. Cheng, B. Cai, K. Yuan, Z. Lian, M. Smietana, P. Lu, D. Liu, Highly-birefringent and ultra-wideband low-loss photonic crystal fiber with rhombic and elliptical holes, Opt. Commun. 450 (2019) 172–175.
[5] C. Tao, H. Wei, W. Feng, Photonic crystal fiber in-line Mach–Zehnder interferometer for explosive detection, Opt Express 24 (2016) 2806–2817.
[6] S. Wu, H. Cheng, J. Ma, X. Yang, S. Wang, P. Lu, Temperature-independent ultra-sensitive refractive index sensor based on hollow-core silica tubes and tapers, Opt Express 29 (2021) 10939–10948.
[7] T. Zhao, S. Lou, X. Wang, W. Zhang, Y. Wang, Simultaneous measurement of curvature, strain and temperature using a twin-core photonic crystal fiber-based sensor, Sensors 18 (2018).
[8] X. Yang, S. Wu, H. Cheng, J. Ma, S. Wang, S. Liu, P. Lu, Simplified highly-sensitive gas pressure sensor based on harmonic Vernier effect, Opt. Laser Technol. 140 (2021) 107007.
[9] K. Naeem, Y. Chung, I.-B. Kwon, Highly sensitive two-dimensional bending vector sensor using an elliptic two-core PCF, IEEE Photonics Technol. Lett. 30 (2018) 273–276.
[10] J. Ma, S. Wu, H. Cheng, X. Yang, S. Wang, P. Lu, Sensitivity-enhanced temperature sensor based on encapsulated S-taper fiber modal interferometer, Opt. Laser Technol. 139 (2021) 106933.
[11] S. Liu, Z. Wang, M. Hou, J. Tian, J. Xia, Asymmetrically infiltrated twin core photonic crystal fiber for dual-parameter sensing, Opt. Laser Technol. 82 (2016) 53–56.
[12] Z. Xu, J.J. Hu, S. Ertman, T. Wolinski, P.P. Shum, Highly sensitive temperature sensor based on hybrid photonic crystal fiber, in: Optical Fiber Communication Conference, 2018.
[13] K. Naeem, B.H. Kim, B. Kim, Y. Chung, High-sensitivity temperature sensor based on a selectively-polymer-filled two-core photonic crystal fiber in-line interferometer, IEEE Sens. J. 15 (2015) 3998–4003.
[14] S. Qiu, J. Yuan, X. Zhou, Y. Qu, B. Yan, Q. Wu, K. Wang, X. Sang, K. Long, C. Yu, Highly sensitive temperature sensing based on all-solid cladding dual-core photonic crystal fiber filled with the toluene and ethanol, Opt. Commun. 477 (2020) 126357.
[15] Zhengyong. Liu, Ming-Leung, Vincent, Tse, Chuang, Wu, Daru, Chen, Chao, Intermodal coupling of supermodes in a twin-core photonic crystal fiber and its application as a pressure sensor, Opt. Express 20 (2012) 21749–21757.
[16] Y.E. Monfared, C. Liang, R. Khosravi, B. Kacerovska, S. Yang, Selectively toluene-filled photonic crystal fiber sagnac interferometer with high sensitivity for temperature sensing applications, Results Phys. 13 (2019) 102297.
[17] E. Sani, A. Dell'Oro, Spectral optical constants of ethanol and isopropanol from ultraviolet to far infrared, Opt. Mater. 60 (2016) 137–141.
[18] L. Jiang, Y. Zheng, L. Hou, K. Zheng, J. Peng, X. Zhao, A novel ultra-broadband single polarization single mode photonic crystal fiber, Opt. Commun. 396 (2017) 8–14.
[19] H. Chen, S. Li, G. An, J. Li, Z. Fan, Y. Han, Polarization splitter based on d-shaped dual-core photonic crystal fibers with gold film, Plasmonics 10 (2014) 57–61.
[20] Khurram, Naeem, Youngjoo, Chung, Bok, Hyeon, Kim, Cascaded two-core PCFs-based in-line fiber interferometer for simultaneous measurement of strain and temperature, Sens. J. IEEE 9 (2019) 1.
[21] J. Zi, S. Li, G. An, Z. Fan, Short-length polarization splitter based on dual-core photonic crystal fiber with hexagonal lattice, Opt. Commun. 363 (2016) 80–84.
[22] P. Madhavan, V. Thamizharasi, M.V. Ranjith Kumar, A. Suresh Kumar, M. Asaduzzaman Jabin, A. Sampathkumar, Numerical investigation of temperature dependent water infiltrated D-shaped dual core photonic crystal fiber (D-DC-PCF) for sensing applications, Results Phys. 13 (2019).
[23] H.L. Chen, S.G. Li, Z.K. Fan, G.W. An, J.S. Li, Y. Han, A novel polarization splitter based on dual-core photonic crystal fiber with a liquid crystal modulation core, IEEE Photonics J. 6 (2014) 1–9.
[24] J. Ma, H.H. Yu, X. Jiang, D.S. Jiang, High-performance temperature sensing using a selectively filled solid-core photonic crystal fiber with a central air-bore, Opt Express 25 (2017) 9406–9415.
[25] Y. Geng, X. Li, X. Tan, Y. Deng, X. Hong, Compact and ultrasensitive temperature sensor with a fully liquid-filled photonic crystal fiber Mach–Zehnder interferometer, IEEE Sens. J. 14 (2014) 167–170.
[26] H. Ademgil, S. Haxha, T. Gorman, F. AbdelMalek, Bending effects on highly birefringent photonic crystal fibers with low chromatic dispersion and low confinement losses, J. Lightwave Technol. 27 (2009) 559–567;
P.S.J. Russell, Photonic-crystal fibers, J. Lightwave Technol. 24 (2006) 4729-4749.